Symmetry Fractionalization

1 Introduction

This lecture is based on review article 'Symmetry Fractionalization in Two Dimensional Topological Phases', arXiv: 1606.07569.

One of the most amazing predictions of topological phases is the existence of fractional excitations. Such excitations can have fractional braiding and fusion statistics when moving around each other. That's where the name 'anyon' came from. However, in experiment, it turns out that these fractional phase factors resulting from braiding are not so easy to observe. Instead, a much more accessible way to see fractionalization is through the fractional quantum number they carry. In, for example, the $\nu = 1/3$ fractional quantum Hall states, the quasi-particles are expected to carry $1/3$ of an electron charge. Theoretically, we can imagine threading a 2π flux through a particular point in the 2D electron liquid and a charge of $e^-/3$ will accumulate around that point.

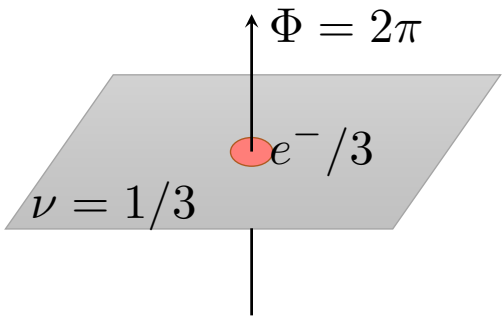

Figure 1: Accumulation of fractional charge $e^-/3$ around a 2π flux in $\nu = 1/3$ fractional quantum Hall state.

And experimentally, this is pretty much what we see [32]. A scan under a single-electron-transistor, as shown in Fig.2, shows three time charing events in the localized states of a $\nu = 1/3$ fractional quantum Hall system as compared to the integer quantum Hall system over the same range of charge density change, therefore confirming the existence of fractional charges.

The $1/3$ charge carried by the quasi-particles in the fractional quantum Hall system is a prototypical example of what we call symmetry fractionalization. Another example of symmetry fractionalization appears in frustrated magnets. In the triangular lattice anti-ferromagnetic Heisenberg model with one spin $1/2$ per lattice site, fractionalization happens due to the frustration of the Heisenberg interaction on different edges. Instead of forming a magnetic or crystal order, the ground state takes the 'resonating valence bond' (RVB) structure, with nearest neighbor pairs of spins forming spin singlets and the ground state wave function being a superposition of all possible pairing configurations.

An excitation in the resonating valence bond state can take the form of an isolated unpaired spin $1/2$'s, each costing a finite amount of energy. The unpairing of certain spins necessarily leads to the reorganization of the pairing of all other spins. However, such a reorganization cannot be

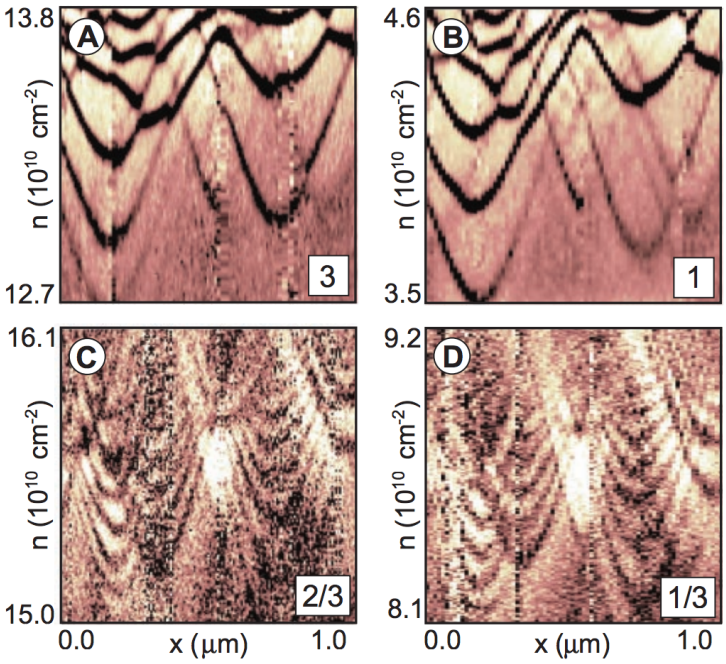

Figure 2: Single electron transistor scan of localized states in integer quantum Hall ((a), (b)) and fractional quantum Hall ((c), (d)) samples with varying charge density and at different positions.

seen locally by looking at the singlet configurations away from the excitations. This is because we started from a superpositions of all possible singlet pairing configurations. When isolated spin 1/2 excitations are created, away from the excitation, locally we still see all possible singlet pairing configurations. Therefore, each isolated spin 1/2 costs only finite energy and can be separated far away from each other.

There are the fractional 'spinon' excitations of the resonating valence bond state and, similar to the quasi-particles in fractional quantum Hall state, they also carry 'fractional quantum numbers' under certain symmetry. In order to talk about fractional quantum number, first we need to say what the 'integer quantum numbers' are. That is, we need to specify what the fundamental degrees of freedom are and how they transform under global symmetry. For the resonating valence bond state, there are two possible descriptions: we can either think of the system as composed of electrons which carry charge e^- and spin 1/2 and be in a Mott-insulating state of one electron per unit cell; or we can think of the system as composed of spin 1/2s on each lattice site. In both cases, the spinon excitation carries 'fractional quantum numbers'.

If we think of the system as composed of electrons and has both charge conservation and spin rotation symmetry, the charge and spin quantum numbers are correlated for any eigenstate of the system. If the state has an odd charge, it then has a half integer spin; if the state has an even charge, it has an integer spin. Therefore, the spin and charge quantum number of any global excitation is also correlated: odd charge half integer spin or even charge integer spin. Compared to the quantum number of the global excitations, the spinons hence carry 'fractional' quantum numbers. In particular, the spinons carry spin 1/2 but no charge (the state with spinon excitation is still a Mott insulating state). This is also called the spin charge separation in strongly correlated electron systems.

On the other hand, if we think of the system as a spin system with spin rotation symmetry, the

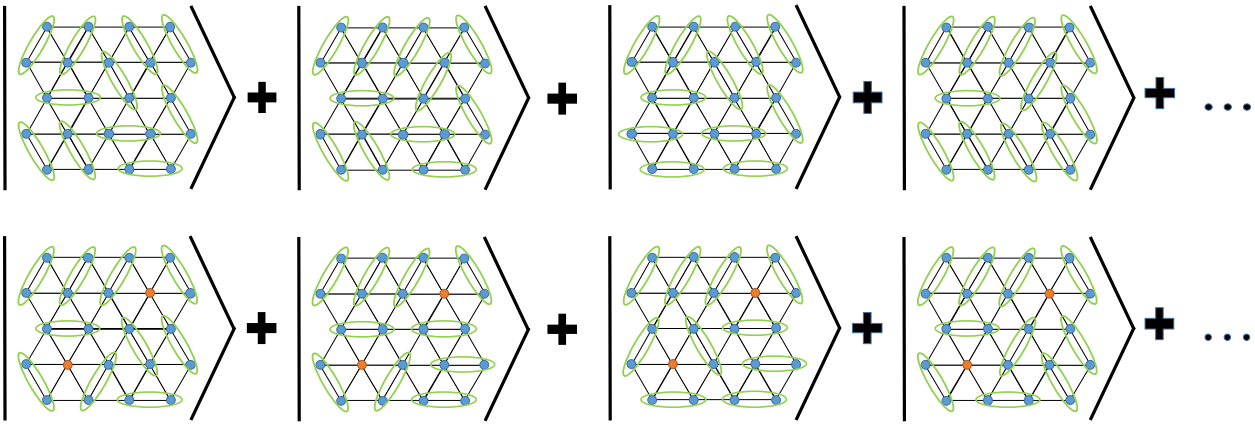

Figure 3: (a) The resonating valence bond wave function is a superposition of all possible singlet pairing configurations. (b) Isolated unpaired spin 1/2's (orange dots) form the spinon excitations of the RVB state.

quantum number carried by the spinon is still fractionalized. This might seem strange because the fundamental degrees of freedoms in the system are spin 1/2's, which carry the same spin quantum number as the spinons. However, if we think about the quantum number of global excitations in the systems, it is always integer spin. No matter whether we have an even or odd number of spin 1/2 in the system, the difference in the representation of different eigenstates is always an integer spin. Therefore, the spin 1/2 representation carried by individual spinons are fractionalized.

This example clearly illustrates the notion of symmetry fractionalization: in 2D topological phases, if the symmetry representation carried by the anyonic excitations is a fraction of that carried by global excitations, then we say there is symmetry fractionalization. Note that SF on anyons is with respect to the symmetry representation carried by global excitations, not that carried by the fundamental degrees of freedom. Even though in some cases, these two coincide.

From the fractional quantum Hall and resonating valence bond state examples we can see that symmetry fractionalization happens in all kinds of topological phases and provides a unique way to probe the nontrivial nature of the system. The question we want to discuss in these lectures is to understand what patterns of symmetry fractionalization can exist and where to find them. As a preparation to answer these questions, we first discuss the important concept of gauging in section 2, which is fundamental to our following discussion of symmetry fractionalization. Section 3 provides the first application of the gauging procedure where interesting SF patterns are obtained by gauging models with global symmetry. With this preparation, we go on to discuss in section 4, a simple consistency condition all SF patterns have to satisfy. That is, they have to be consistent with the fusion rules of the anyons. We are going to explain the meaning of this condition and how this leads to a complete –in some sense over-complete– list of possible SF patterns. It is over complete because, surprisingly, not all consistent SF patterns can be realized in strictly 2D systems. Such SF patterns are called 'anomalous'. If two dimensional models can be constructed to realize a particular SF pattern, as illustrated in section 5 using lattice model or Chern Simon field theory, then the SF pattern is not anomalous. Of course, it is not always obvious how to construct such models or if it is possible at all! In section 6, we discuss examples of anomalous SF patterns which are in principle not possible in 2D and various methods devised to detect such anomalies. With the preparation in section 4 and 6, one can then perform a systematic study of SF patterns that can be realized in 2D topological phases with symmetry, the so-called Symmetry Enriched Topological phases. We discuss in section 7 the case of spin liquids, i.e. frustrated spin

models with certain topological order and various symmetries like spin rotation, time reversal and lattice symmetries. A list of potentially realization SF patterns can be obtained by excluding the anomalous SF patterns from all consistent ones. It is then interesting to ask which one of them is realized in simple physical models, e.g. the Kagome lattice Heisenberg model. Numerical and experimental probe methods have been proposed which we also review in section 7. On the other hand, the anomalous SF patterns are not completely impossible. While they cannot be realized in strictly 2D systems, they can appear on the 2D surface of a 3D system. The anomaly in the SF pattern is tightly connected to the nontrivial order in the 3D bulk and we discuss various examples of such connections in section 8.

2 Gauging

Before we start to discuss symmetry fractionalization in general, I want to first explain in detail the idea of 'gauging'. This will not only lead to some simple examples of SF patterns, but also provide a powerful tool throughout the study of all SF patterns.

In our discussion, 'gauging' means coupling a quantum mechanical system with certain global symmetry to the corresponding dynamical gauge field in the deconfined phase. For example, we can consider an Ising paramagnet (at zero temperature) with global Z_2 symmetry and couple it to a Z_2 gauge field.

In the transverse field Ising model, the Hamiltonian at the paramagnetic limit (no spontaneous symmetry breaking) takes the simple form of

$$H = -\sum_i \sigma_i^x \tag{1}$$

where σ^x acts on the spin 1/2 degrees of freedom on each lattice site (blue dots in Fig.4) as $\begin{pmatrix} 0 & 1 \\ 1 & 0 \end{pmatrix}$. The system has a global Z_2 symmetry of $U = \prod_i \sigma_i^x$ and the ground state is invariant under this symmetry

$$|\psi\rangle = \otimes \frac{1}{\sqrt{2}} (|\uparrow\rangle + |\downarrow\rangle) \tag{2}$$

where $|\uparrow\rangle$ and $|\downarrow\rangle$ are eigenstates of $\sigma_z = \begin{pmatrix} 1 & 0 \\ 0 & -1 \end{pmatrix}$.

One result of gauging is to take a system with global symmetry and turn it into a system with local symmetry. That is, the symmetry group will be generated not by just one global symmetry operation, but by symmetry operations at all spatial locations (on each lattice site). To do this, first we introduce the gauge field degrees of freedom on each link of the lattice (yellow diamonds in Fig.4). For a Z_2 gauge field, the degrees of freedom are again two level spin 1/2's and we label them as τ spins. The local Z_2 symmetry acts as $U_i = \sigma_i^x \prod_{i\in e} \tau_e^x$ where the product is over all edges with i as one end point.

This local symmetry can be interpreted as enforcing the Gauss law on the gauge field. Using the terminology in electromagnetism, the τ^z operator corresponds to the vector potential A of the gauge field, actually the exponential of it e^{iA}. As this is a Z_2 gauge field, A only takes discrete value of $n\pi, n \in \mathbb{Z}$. The operator τ^x on the other hand corresponds to the exponential of the electric field e^{iE}. Similarly, the electric field takes only discrete value. The quantum-ness

of the gauge field is manifested in the fact that the electric field and the vector potential do not commute. As σ_i^x measures the amount of Z_2 charge on each lattice site, the local symmetry operator $U_i = \sigma_i^x \prod_{i\in e} \tau_e^x = \sigma_i^x e^{i\sum_{i\in e} E_e}$ is equivalent to the Gauss law which says that the amount of charge at each site is equal to the integral of the electric field on a surrounding surface.

Next, we write down a new Hamiltonian which is invariant under the local symmetry transformations and also captures the dynamics of the gauge field. For the Ising paramagnetic model above, the Hamiltonian terms σ_i^x are already invariant under the local symmetries, so we do not need to do anything about them and just include them in the new Hamiltonian. Generically, this is not the case. For example, if (small) nearest neighbor Ising coupling terms $\sigma_i^z\sigma_j^z$ are in the Hamiltonian, they need to be modified as $\sigma_i^z\tau_{ij}^z\sigma_j^z$ in order to be invariant under all local symmetry transformations.

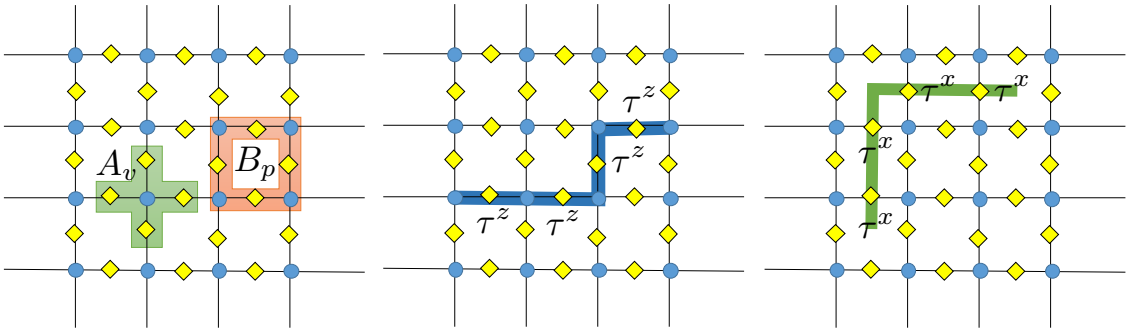

Figure 4:

Besides that we add the term $A_v = \sigma_v^x \prod_{v\in e} \tau_e^x$ at every vertex v to enforce gauge symmetry (Gauss law) and $B_p = \prod_{e\in p} \tau_e^z$, where the product is over all edges around a plaquette p, to enforce zero flux constraint on every plaquette. The total Hamiltonian then reads

$$H_g = -\sum_i \sigma_i^x - \sum_v A_v - \sum_p B_p = -\sum_i \sigma_i^x - \sum_v \sigma_v^x \prod_{v\in e} \tau_e^x - \sum_p \prod_{e\in p} \tau_e^z \tag{3}$$

In a pure gauge theory, A_v is enforced as a constraint, or equivalently the weight of this term is taken to be $+\infty$. In this limit, the Hamiltonian can be simplified into

$$H_g = -\sum_v \prod_{v\in e} \tau_e^x - \sum_p \prod_{e\in p} \tau_e^z \tag{4}$$

which is exactly the toric code Hamiltonian.

There are two types of excitations in the gauged Hamiltonian: a charge excitation e and a flux excitation m. A charge excitation e is a violation of the A_v term, which is equivalent to a violation of the σ_x term which measures onsite symmetry charges, and a flux excitation m is a violation of the B_p term. These two types of excitations can be generated in pairs using string operators $\prod_{e\in S} \sigma_e^z$ and $\prod_{e\in \tilde{S}} \sigma_e^x$, as shown in Fig.4, where S and $\tilde{S}$ are paths on the lattice and dual lattice respectively. The gauge charge is a bosonic anyon, corresponding to the spin flip of the σ spins. The gauge flux is is also a bosonic anyon. They braid with each other with a phase factor of -1 which is the Aharonov-Bohm phase factor in the Z_2 case ($e^{i\pi}$). The composite of e and m is hence a fermion, usually denoted as f.

This gauging procedure can be generalized to all kinds of global internal unitary symmetries of group G in the following steps:

1. Take a system with global unitary internal symmetry of group G with degrees of freedom on the sites of a lattice and with global symmetry acting as a tensor product of operator on each lattice site.
2. Introduce gauge field degrees of freedom onto the links of the lattice and define gauge symmetry transformation as acting on each lattice site and the links around it.
3. Modify the terms in the original Hamiltonian, by coupling the original degrees of freedom with the gauge field, such that each term is invariant under all local gauge symmetry transformations.
4. Add vertex terms to the Hamiltonian to enforce gauge symmetry and add plaquette terms to enforce the zero flux constraint.

By doing so, we obtain a gauge theory of group G with gauge charge and gauge flux excitations. There are a few things we can learn from the gauging procedure:

1. The gauge charge comes from the symmetry charge. They are labeled by the representation of the group, are either a bosonic or a fermionic anyon, depending on whether the symmetry charges in the original system are bosonic or fermionic.
2. The gauge flux comes from the symmetry flux and are labeled by the group elements of G (conjugacy classes if G is nonabelian). The statistics of the gauge flux is more complicated. It depends on the particular order (symmetry protected / symmetry enriched topological order) of the original Hamiltonian. If the original Hamiltonian does not have nontrivial order (ground state can be a total product state), the gauge fluxes are bosonic.
3. The braiding statistics between a gauge charge and a gauge flux is independent of the original order. It is given by the Aharonov-Bohm phase factor.

We are going to explain more about the second point on the connection between gauge flux and symmetry flux in section 6.

3 SF pattern from gauging

Using this gauging procedure, we can find simple symmetry fractionalization patterns for a gauge theory. Consider for example the Ising paramagnet discussed above. We can think of the σ degrees of freedom as representing the Hilbert space of a hard core boson. $\frac{1}{\sqrt{2}}(|\uparrow\rangle + |\downarrow\rangle)$ corresponds to no boson and $\frac{1}{\sqrt{2}}(|\uparrow\rangle - |\downarrow\rangle)$ corresponds to one boson. The Z_2 symmetry of $U = \prod_i \sigma_i^x$ then measures the boson number parity. The bosons are then symmetry charges under the Z_2 symmetry and upon gauging, they become the gauge charges. Now imagine that each boson has its own internal structure in the form of a pseudo-spin degree of freedom ρ which forms a spin 1/2 representation under pseudo-spin rotation. Correspondingly, the gauge charge in the gauged model also transforms as a spin 1/2. With this mapping, the gauged Ising paramagnet model has the same symmetry fractionalization pattern as the RVB model – they both have toric code type Z_2 topological order and the gauge charge transforms as a spin 1/2.

Following this construction, it is then easy to see that in a gauge theory, the gauge charge can transform in a variety of fractional ways: carry fractional pseudo-charge, being a half integer

pseudo-spin, transform as a Kramer doublet under time reversal ($\mathcal{T}^2 = -1$), etc. All we need to do is to start from a matter field (boson or fermion) carrying charge 1 under a $U(1)$ symmetry or a discrete subgroup of it (e.g. Z_2). At the same time the matter field carries some fractional quantum number / symmetry representation under pseudo-charge, pseudo-spin symmetry etc. Put the matter field into a Mott insulator type of state and couple it to the dynamical gauge field of the charge $U(1)$ group (or a discrete subgroup of it). By doing so, we would obtain a gauge theory with gauge charge transforming in a fractional way under pseudo-charge or pseudo-spin symmetries. In this case, the gauge flux always transforms in a trivial (non-fractional) way.

Can gauge flux also transform in a fractional way? In order to achieve that, the matter field has to have some nontrivial gapped symmetric order (as compared to a Mott insulator). Let's consider the example of gauging the fermion parity symmetry in a topological superconductor. The topological superconductor can be thought of as composed of a $p + ip$ superconductor of spin up and a $p - ip$ superconductor of spin down. It is invariant under both the fermion parity symmetry P_f and the time reversal symmetry $\mathcal{T}$ and $\mathcal{T}^2 = P_f$. If the fermion parity symmetry, as a unitary global Z_2 symmetry, is gauged, we obtain a Z_2 gauge theory with time reversal symmetry and we want to know how the gauge charge and gauge flux transform under time reversal.

The gauge charge f, which follows from the symmetry charge in the topological superconductor, is a fermion. It transforms under time reversal as $\mathcal{T}^2 = -1$. The gauge flux e transforms in a more nontrivial way. First, let's find out what kind of anyon the gauge flux is. To see this, note that the topological superconductor is equivalent to a simple s-wave superconductor if time reversal symmetry can be broken. That is to say, if we forget about time reversal symmetry and just ask about the statistics of the gauged theory, topological superconductor and s-wave superconductor should give the same result. In particular, they both have bosonic gauge fluxes. The topological order of the gauged theory is equivalent to that of the toric code and we have already adopted the notation for the anyons. The difference from our previous discussion of toric code as a Z_2 gauge theory is that the gauge charge in this case is a fermion, while the composite of the gauge charge and the gauge flux $e = fm$ is a boson.

To understand how the gauge flux transform under time reversal symmetry, we can think about the transformation of the π flux in a topological superconductor. The π flux in the topological superconductor is a confined defect, which upon gauging becomes the deconfined gauge flux of the Z_2 gauge theory. The transformation property under time reversal symmetry also carries over. In a $p + ip$ or $p - ip$ superconductor, a π flux carries a Majorana mode. Therefore, in a topological superconductor, a π flux carries two Majorana modes $\gamma_\uparrow$ and $\gamma_\downarrow$. $\gamma_\uparrow$ and $\gamma_\downarrow$ make up a two dimensional Hilbert space of a complex fermion mode with fermion parity operator being $P = i\gamma_\uparrow\gamma_\downarrow$. Time reversal maps $\gamma_\uparrow \to \gamma_\downarrow$, $\gamma_\downarrow \to -\gamma_\uparrow$, and $i \to -i$ and hence reverses fermion parity $P \to -P$. That is to say, time reversal adds / removes a fermion from the π flux. After gauging, this is saying that time reversal maps between e and m in the Z_2 gauge theory. Therefore, the gauged topological superconductor provides a highly nontrivial example of symmetry fractionalization where time reversal exchanges two types of anyon.

In our following discussion, we are going to focus on the simple type of symmetry fractionalization where anyon types are not changed. With the gauged topological superconductor, we want to discuss at least one example where symmetry does change anyon type.

Taking a system with certain global symmetry and partially gauging it can result in gauge theories with gauge charge and gauge flux transforming in a nontrivial way. But of course, not all topological orders are gauge theories. Even for gauge theory, it is not clear if all patterns of symmetry

fractionalization can be realized by gauging a symmetric model. Therefore, in order to understand what SF patterns are possible and what are not, we need a more general theory.

4 Consistency Condition

Given a topological order, with its full anyon content and their fusion and braiding rules, and certain global symmetry, what SF patterns are possible? For an SF pattern to be possible, it first has to satisfy some consistency conditions.

To understand the consistency condition the SF patterns have to satisfy, let's go back to the $\nu = 1/3$ fqH example. The elementary anyonic excitation in the system can be thought of as $1/3$ of an electron. That is, if we put three of them together, they are equivalent to a single electron excitation. Therefore, the amount of charge they each carry has to be $1/3$ of an electron charge. If they were to carry any other different fractional amount of charge (like $1/2$ or $1/5$), it will not be consistent. Similarly, in the case of spin-charge separation, the combination of a spinon and a chargon is equivalent to a single electron. This is consistent with the SF pattern on the spinons and chargons, as the sum of their charge / spin quantum numbers equals that of a single electron. Such a consistency condition can be readily generalized to all 2D anyon theories. To present this consistency condition, we need to introduce the concept of projective symmetry action on the anyons.

Consider a 2D topological phase containing anyon types a, b, c etc. and with global symmetry of group G. The ground state, which has a finite energy gap to all the excited states, is invariant under global symmetry action. Now imagine creating a pair of anyons a and $\bar{a}$ and moving them to distant locations, as shown in Fig.5. If we apply global symmetry $g \in G$ to the system, everywhere away from the anyons the system remains invariant as the state is the same as in the ground state, while near the anyons the system may be transformed in a nontrivial way. If the symmetry g does not change anyon types (which is the case we focus on in this lecture), then the transformation is equivalent to some local unitaries $U_a(g)$ and $U_{\bar{a}}(g)$ near the anyons, as shown in Fig.5. That is to say, global symmetry action on a state with isolated anyons can be reduced to symmetry actions on each anyon individually.

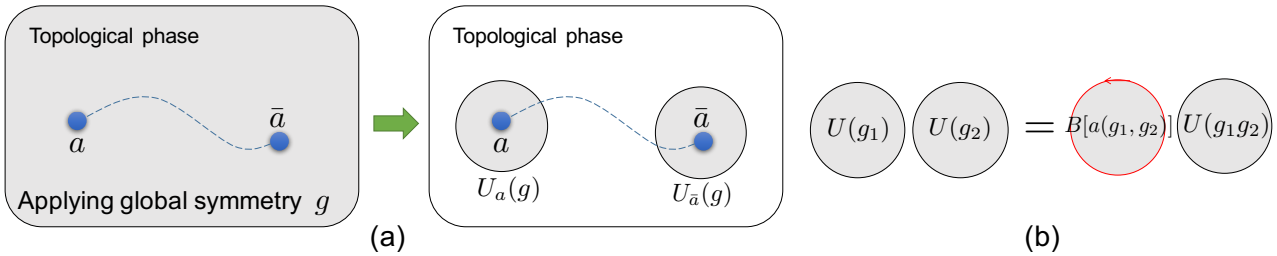

Figure 5: (a) Global symmetry action on a state with isolated anyons can be reduced to symmetry actions on each anyon individually, (b) which form a 'projective' representation of the group.

These local symmetry transformations are special in that they only have to satisfy the group relation up to a phase. That is,

$$U_a(g_1)U_a(g_2) = \omega_a(g_1, g_2)U_a(g_1g_2) \tag{5}$$

where $\omega_a(g_1, g_2)$ is a phase factor that is not necessarily 1. $U_a(g)$ is said to form a 'projective'

representation of group G.This is not contradicting to the global symmetry of the system as long as the phase factor on $\bar{a}$ – $\omega_{\bar{a}}(g_1, g_2)$ – cancels with $\omega_a(g_1, g_2)$. On the other hand, on any global excitation, ω has to be 1 and $U(g)$ is said to form a 'linear' representation on these non-fractionalized excitations. For example, if we apply two consecutive π rotations in the $U(1)$ symmetry group of charge conservation to the 1/3 electron excitation in the $\nu = 1/3$ fqH, we get

$$U_{1/3}(\pi)U_{1/3}(\pi) = e^{i2\pi/3}U_{1/3}(0) \tag{6}$$

Note that as two excitations related to each other through local operations are considered to be of the same anyon type, two projective representations differing by a linear representation correspond to the same SF pattern, as described by the same ω. In the fqH case, this tells us that only the fractional part of the charge carried by the anyon matters.

The associativity condition that $(U_a(g_1)U_a(g_2))\,U_a(g_3) = U_a(g_1)\,(U_a(g_2)U_a(g_3))$ leads to the requirement that

$$\omega_a^{s(g_1)}(g_2, g_3)\omega_a(g_1, g_2g_3) = \omega_a(g_1, g_2)\omega_a(g_1g_2, g_3), \tag{7}$$

which needs to be satisfied by any ω describing a projective symmetry action. Moreover we have the freedom to change the definition of each $U_a(g)$ by an arbitrary phase factor $\mu_a(g)$. Therefore, $\omega_a(g_1, g_2)$ and $\omega'_a(g_1, g_2)$ related as

$$\omega'_a(g_1, g_2) = \frac{\mu_a(g_1)\mu_a^{s(g_1)}(g_2)}{\mu_a(g_1g_2)}\omega_a(g_1, g_2) \tag{8}$$

are considered equivalent. Here $s(g_1) = 1$ if g_1 is unitary and $s(g_1) = -1$ if g_1 is anti-unitary (time reversal). Eq.7 and 8 defines the equivalence classes of projective representations, which is an essential concept in the consistency condition of SF patterns discussed below.

The consistency condition of SF patterns then states that: *if c is (one of) the fusion product of a and b, then the projective representation carried by c should be equivalent to the tensor product of that carried by a and b.* That is, if the anyons obey fusion rules $a \times b = \sum_c N_{ab}^c c$, then when $N_{ab}^c \neq 0$,

$$\omega_a(g_1, g_2)\omega_b(g_1, g_2) \sim \omega_c(g_1, g_2) \tag{9}$$

Here we are using '$\sim$' instead of '$=$' because the ω's only have to be equivalent as describe in Eq.8. In the $\nu = 1/3$ fqH case, this condition is simply saying that the fractional part of the charge carried by three elementary excitations should sum to one.

What is the physical meaning of this projective phase factor ω? It turns out that ω relates the local action of symmetry to anyon braiding statistics. Consider again the $\nu = 1/3$ fqH example. Applying two consecutive π rotations to a region D is equivalent to doing nothing up to a phase factor. The phase factor is $e^{i2\pi n/3}$ if we have n elementary anyons in the region D. On the other hand, this is exactly the phase factor induced by braiding an elementary anyon around this region D, as shown in Fig.5. Therefore, we have the following relation

$$U(\pi)U(\pi) = B[a_{1/3}]U(0) \tag{10}$$

where $B[a_{1/3}]$ denotes the braiding of the 1/3 electron around region D. Note that this relation holds no matter what the anyon content is in the region D. In general, we have

$$U(g_1)U(g_2) = B[a(g_1, g_2)]U(g_1g_2) \tag{11}$$

where $a(g_1, g_2)$ takes value in the set of abelian anyons of the system which we denote as A. $B[a(g_1, g_2)]$ denotes the braiding of $a(g_1, g_2)$ around region D, such that $\omega_b(g_1, g_2)$ is equal to the braiding statistics between b and $a(g_1, g_2)$. It is easy to check that the set of projective representations carried by the anyons (as described by ω) generated in this way automatically satisfy the consistency condition described above, due to the additivity of braiding statistics with abelian anyons. Here we are discussing the local symmetry action $U(g)$ in an abstract way. In section **??** we are going to discuss explicitly how to find the operator $U(g)$ for a gapped symmetric state and why they satisfy the relation in Eq. 11.

Equation 11 hence describes the SF patterns on all the anyons in the topological phase together. We can interpret the $U(g)$'s in Eq.11 as a projective representation of the symmetry group G, but not with coefficient in phase factors as in the case of $U_a(g)$, but rather with coefficient in A, the set of abelian anyons of the system. The conditions the abelian anyon coefficient $a(g_1, g_2)$ has to satisfy is completely analogous to that for the phase factor coefficient $\omega_a(g_1, g_2)$. First, associativity requires that

$$a(g_2, g_3) \times a(g_1, g_2 g_3) = a(g_1, g_2) \times a(g_1 g_2, g_3), \tag{12}$$

Here '$\times$' denotes fusion of abelian anyons. Two sets of anyon coefficient are equivalent if they can be related as

$$a'(g_1, g_2) = b(g_1) \times b(g_2) \times \bar{b}(g_1 g_2) \times a(g_1, g_2) \tag{13}$$

where for any choice of $b(g) \in A$. This relation comes from redefining the local symmetry action $U(g)$ by braiding $b(g)$ around the region. Using Eq. 12 and 13, we can then find all possible and distinct SF patterns. Mathematically speaking, the set of SF patterns is classified by the second cohomology group of G with coefficient in abelian anyons A, denoted as $H^2(G, A)$. This result can be generalized to the situation where anyon types are permuted under symmetry transformation, as discussed in [2, 53].

Note that while the above discussion is based on internal symmetries like spin rotation or time reversal, it can be applied to spatial symmetries as well. Consider, for example, the case of reflection symmetry R. Imagine creating a pair of anyons a and $\bar{a}$. If a is the same as $\bar{a}$, this can be done in a way that preserves reflection symmetry. One can then decompose the action of reflection symmetry as spatially exchanging the position of the two a's, together with some local unitaries $U_a(R)$ around each of the a's. $U_a(R)$ then effectively acts as a internal Z_2 symmetry on a and its possible fractionalization patterns follow from that of Z_2.

Let's see apply the above classification conclusion to the case of a Z_2 spin liquid with time reversal symmetry. A spin liquid with Z_2 topological order contains four abeilan anyons $\{\mathbb{I}, e, m, f\}$. If the system has global time reversal symmetry, which satisfies $\mathcal{T}\mathcal{T} = I$, locally the symmetry action may act as

$$U(\mathcal{T})U^*(\mathcal{T}) = B[a(\mathcal{T}, \mathcal{T})], \quad a(\mathcal{T}, \mathcal{T}) = \mathbb{I} \text{ or } e \text{ or } m \text{ or } f \tag{14}$$

Note that the second $U(\mathcal{T})$ is complex conjugated because the first symmetry action is anti-unitary. These four cases exhaust all possible SF patterns in the Z_2 spin liquid and they are not related to each other through Eq.13. What does this mean physically? Suppose that $U(\mathcal{T})U^*(\mathcal{T}) = e$. This is saying that applying time reversal twice on m or f gives -1, while applying time reversal twice on $\mathbb{I}$ or e gives $+1$. That is, the anyons m and f transform as a Kramer doublet under time reversal and anyon e (and the vacuum $\mathbb{I}$) transform as a singlet.

One can apply this procedure to spin liquids with all kinds of symmetries and completely list all consistent SF patterns. For example, in [14], this procedure has been carried out for Z_2 spin

liquid with square lattice space group, time reversal and $SO(3)$ spin rotation symmetries, where 2^{21} different types of SF patterns where identified.

So there is a huge number of SF patterns that satisfy the consistency condition. Can they all be realized in local two dimensional systems?

5 Construction of SF patterns in 2D

If we can construct explicit 2D models to realize certain SF pattern, then of course, it is non-anomalous. Models can be constructed either on the lattice or using field theory.

5.1 SF pattern in lattice model

Some SF patterns of the toric code model can be realized with simple lattice construction.

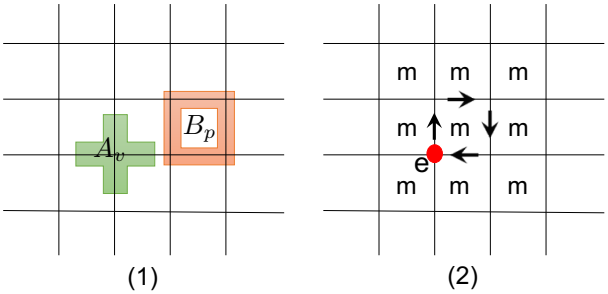

Figure 6: (1) Toric code Hamiltonian on the square lattice (2) Gauge charge moving in the background of π fluxes in each plaquette.

Consider the original toric code Hamiltonian on a square lattice

$$H = -\sum_v \prod_{v\in e} \tau_e^x - \sum_p \prod_{e\in p} \tau_e^z \tag{15}$$

as shown in Fig.6 (1). This model has translation symmetry in both x and y directions. The anyons e and m transform under translation symmetry in a pretty normal way: they move from one vertex to another vertex, or from one plaquette to another plaquette.

Now let's switch the sign of one of the terms

$$H = -\sum_v \prod_{v\in e} \tau_e^x + \sum_p \prod_{e\in p} \tau_e^z \tag{16}$$

Because of the this, it is energetically preferable to have an m anyon in each plaquette, as shown in Fig.6 (2). That is, each plaquette contains a gauge flux of the Z_2 gauge field in the group state. The motion of the gauge charge is then affected by this background flux. In particular, if e moves around a plaquette, it acquires a phase factor of -1. That is to say

$$T_e(x)T_e(y)T_e^{-1}(x)T_e^{-1}(y) = -1 \tag{17}$$

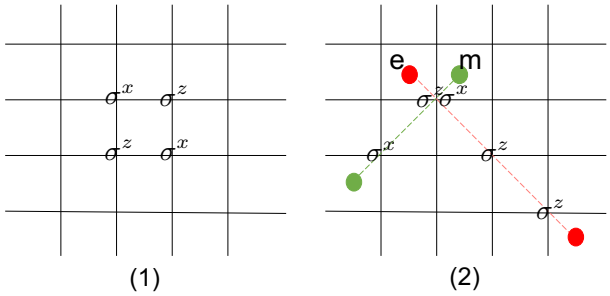

Figure 7: (1) A variant of Toric code on square lattice with degrees of freedom on vertices and the same Hamiltonian term in each plaquette (2) Gauge charge and gauge flux correspond to excitations in neighboring plaquettes.

or equivalently, translation in x direction anti-commutes with translation in y direction. This example illustrates one of the key ideas of string-flux construction discussed in [21].

Let's consider a different model of Z_2 gauge theory where translation symmetry acts on the anyons in a different way. Consider the square lattice as shown in Fig.7 which lattice site has a spin 1/2 degree of freedom. The Hamiltonian is a sum of terms in each plaquette

$$H = -\sum_{<i,j>} \sigma^x_{i,j}\sigma^z_{i,j+1}\sigma^z_{i+1,j}\sigma^x_{i+1,j+1} \tag{18}$$

As shown in Fig.7, a diagonal string of σ^x creates the gauge charge excitations and a diagonal string of σ^z originating from a neighboring plaquette creates the gauge flux excitations. Therefore, translation symmetry from one plaquette to another exchanges e and m.

5.2 SF pattern in Chern-Simons theory

Another useful tool in the study of symmetry fractionalization is the Chern-Simons formalism. It provides a particularly simple framework for studying abelian topological phases and the symmetry transformation of their anyons.

An abelian topological order is described using the Chern-Simons field theory with Lagrangian

$$\mathcal{L} = \frac{1}{4\pi} K_{IJ}\epsilon^{\lambda\mu\nu} a_{I\lambda}\partial_\mu a_{J\nu} \tag{19}$$

of a p-component gauge field a_I. The matrix K is a $p\times p$ symmetric, non-degenerate integer matrix. Anyon excitations of the theory are described by a p-component integer vector l. The topological spin of the anyon labeled by l is

$$\theta_l = \pi l^T K^{-1} l \tag{20}$$

The full braiding statistics between anyons labeled by l and l' is

$$\theta_{ll'} = 2\pi l^T K^{-1} l' \tag{21}$$

The ground state degeneracy on a torus, hence the total number of anyon types, is given by $\det(K)$ and the chirality is given by the difference in the number of positive and negative eigenvalues of K.

For example, the Z_2 toric code is described by $K = \begin{pmatrix} 0 & 2 \\ 2 & 0 \end{pmatrix}$. The gauge charge e corresponds to $l = \begin{pmatrix} 1, 0 \end{pmatrix}^T$ and the gauge flux m corresponds to $l = \begin{pmatrix} 0, 1 \end{pmatrix}^T$. The chiral semion theory is described by $K = 2$ and the semionic anyon corresponds to $l = 1$.

Correspondingly, the edge of the system can be described as

$$\mathcal{L}_e = \frac{1}{4\pi} K_{IJ} \partial_x \phi_I \partial_t \phi_J \tag{22}$$

where ϕ is a p-component field, with each component being a 2π periodic scalar field. Anyon excitations are given by $e^{il^T\phi}$.

Symmetry transformation of this topological state, and in particular symmetry transformation on the anyons, can be conveniently described in terms of the symmetry transformation of the ϕ field. Under symmetry action, the ϕ field transformations as

$$\phi \to W \times \phi + \delta\phi \tag{23}$$

where W is a $p \times p$ integer matrix and $\delta\phi$ is a p-component vector. The theory is invariant under the symmetry transformation if

$$W^T K W = W \tag{24}$$

for unitary symmetry and

$$W^T K W = -W \tag{25}$$

for anti-unitary symmetry (time reversal).

Using this formalism, we can easily write down theories with different symmetry fractionalization patterns.

For example, consider a toric code type Z_2 gauge theory with Z_2 unitary symmetry. An SF pattern with gauge charge e carrying a fractional Z_2 charge and gauge flux m carrying an integer Z_2 charge can be realized as

$$\phi_1 \to \phi_1 + \pi/2, \ \phi_2 \to \phi_2 \tag{26}$$

such that the anyon creation operators transform as

$$e^{i\phi_1} \xrightarrow{Z_2} ie^{i\phi_1} \xrightarrow{Z_2} -e^{i\phi_1}, e^{i\phi_2} \xrightarrow{Z_2} e^{i\phi_2} \xrightarrow{Z_2} e^{i\phi_2} \tag{27}$$

The W matrix is the 2×2 identity matrix and satisfies $W^T K W = K$.

An SF pattern with gauge charge e carrying a fractional Z_2 charge and gauge flux m also carrying a fractional Z_2 charge can be realized as

$$\phi_1 \to \phi_1 + \pi/2, \ \phi_2 \to \phi_2 + \pi/2 \tag{28}$$

such that the anyon creation operators transform as

$$e^{i\phi_1} \xrightarrow{Z_2} ie^{i\phi_1} \xrightarrow{Z_2} -e^{i\phi_1}, e^{i\phi_2} \xrightarrow{Z_2} ie^{i\phi_2} \xrightarrow{Z_2} -e^{i\phi_2} \tag{29}$$

An SF pattern with the Z_2 symmetry exchanging e and m can be realized as

$$\phi_1 \to \phi_2, \phi_2 \to \phi_1 \tag{30}$$

such that the anyon creation operators transform as

$$e^{i\phi_1} \xrightarrow{Z_2} e^{i\phi_2} \xrightarrow{Z_2} e^{i\phi_1}, e^{i\phi_2} \xrightarrow{Z_2} e^{i\phi_1} \xrightarrow{Z_2} e^{i\phi_2} \tag{31}$$

Similar construction works for time reversal symmetry. An SF pattern with gauge charge e transforming as $\mathcal{T}^2 = 1$ and the gauge flux transforming as $\mathcal{T}^2 = -1$ can be realized as

$$\phi_1 \to -\phi_1, \phi_2 \to \phi_2 + \pi/2 \tag{32}$$

such that the anyon creation operators transform as

$$e^{i\phi_1} \xrightarrow{\mathcal{T}} e^{i\phi_1} \xrightarrow{\mathcal{T}} e^{i\phi_1}, e^{i\phi_2} \xrightarrow{\mathcal{T}} -ie^{-i\phi_2} \xrightarrow{\mathcal{T}} -e^{i\phi_2} \tag{33}$$

Here $W = \begin{pmatrix} -1 & 0 \\ 0 & 1 \end{pmatrix}$ and $W^T K W = -K$.

Is it possible to have an SF pattern where both e and m transform as $\mathcal{T}^2 = -1$? We can try to assign the ϕ fields to transform as

$$\phi_1 \to \phi_1 + \pi/2, \ \phi_2 \to \phi_2 + \pi/2 \tag{34}$$

such that the anyon creation operators transform as

$$e^{i\phi_1} \xrightarrow{\mathcal{T}} -ie^{-i\phi_1} \xrightarrow{\mathcal{T}} -e^{i\phi_1}, e^{i\phi_2} \xrightarrow{\mathcal{T}} -ie^{-i\phi_2} \xrightarrow{\mathcal{T}} -e^{i\phi_2} \tag{35}$$

However, in this case the W matrix is I which commutes with K. Therefore, the above transformation actually describes a unitary Z_2 symmetry, not a time reversal symmetry. Is it then possible, at all, to have an SF pattern where both e and m transform as $\mathcal{T}^2 = -1$?

Similarly, we can ask is it possible to have an SF pattern where time reversal exchanges e and m? We can try to assign the ϕ fields to transform as

$$\phi_1 \to -\phi_2, \ \phi_2 \to -\phi_1 \tag{36}$$

such that the anyon creation operators transform as

$$e^{i\phi_1} \xrightarrow{\mathcal{T}} e^{i\phi_2}, e^{i\phi_2} \xrightarrow{\mathcal{T}} e^{i\phi_1} \tag{37}$$

However, in this case the W matrix is $\begin{pmatrix} 0 & -1 \\ -1 & 0 \end{pmatrix}$ which commutes with K. Therefore, the above transformation is unitary. This is the same unitary Z_2 symmetry as we discussed above which exchanges e and m.

Instead, we can try to assign the ϕ fields to transform as

$$\phi_1 \to \phi_2, \ \phi_2 \to -\phi_1 \tag{38}$$

The W matrix is now $\begin{pmatrix} 0 & 1 \\ -1 & 0 \end{pmatrix}$ which satisfies $W^T K W = -K$. However, the anyon creation operators transform as

$$e^{i\phi_1} \xrightarrow{\mathcal{T}} e^{-i\phi_2} \xrightarrow{\mathcal{T}} e^{-i\phi_1}, e^{i\phi_2} \xrightarrow{\mathcal{T}} e^{i\phi_1} \xrightarrow{\mathcal{T}} e^{-i\phi_2} \tag{39}$$

Therefore, after applying time reversal twice, each anyon is changed by adding a local excitation $e^{-2i\phi_1}$ or $e^{-2i\phi_2}$, which is not an identity operation.

Both construction fails, but in fact we already know that time reversal exchanging e and m can happen, from our discussion of gauged topological superconductor. Therefore, the Chern-Simons approach is powerful, but it also has its limitation. It allows us to construct a variety of SF patterns. However, for those which the construction fails, there are two possibilities. 1. the SF pattern is anomalous and cannot be realized in pure 2D systems; 2. the SF pattern is possible in 2D, although not covered in the simplest version of Chern-Simon theory we discussed above. To distinguish between these cases and identify true anomaly in SF patterns, we are going to discuss anomaly and its detection methods below in a model independent way.

6 Anomaly Detection

One important realization about symmetry fractionalization is that, among all the consistent SF patterns, not every one can be realized in strictly 2D systems. The ones that cannot are said to be 'anomalous'. At first sight this may seem surprising, as the consistent SF patterns (for example the four possibilities for time reversal in Z_2 spin liquid) look very much well-behaved and there seems to be no particular reason to suspect that one is more exotic than another. In fact, one has to look very carefully to see the distinction. In this section, we first give some examples of how such anomalies can occur, and then introduce a number of methods that have been developed to detect anomalies in this situation. These methods are all based on the powerful idea of 'gauging'.

6.1 Anomalous SF Pattern: Examples

Consider a system with Z_2 topological order and charge conservation symmetry. The SF pattern is given by the fractional charge carried by the anyons e, m and f. Note that we are always talking about the charge amount mod 1, as the integer part of the charge does not matter. One consistent SF pattern is that e and m carry charge $1/2$ while f carries charge 0. In terms of the projective representation formed by local symmetry operations as given in Eq.11, we have

$$a(\theta, 2\pi - \theta) = f, \quad a(\theta_1, \theta_2) = \mathbb{I} \text{ otherwise} \tag{40}$$

This SF pattern has a name – $eCmC$. This SF pattern can be realized in strictly 2D systems, as can be seen from the Chern-Simons theory description with $K = \begin{pmatrix} 0 & 2 \\ 2 & 0 \end{pmatrix}$ and the ϕ fields transforming under charge conservation symmetry as

$$\phi_1 \xrightarrow{\alpha} \phi_1 + \alpha/2, \phi_2 \xrightarrow{\alpha} \phi_2 + \alpha/2, \tag{41}$$

where α labels the $U(1)$ symmetry transformation of charge conservation. With this $U(1)$ symmetry, we can couple the system to external $U(1)$ gauge field (electro-magnetic field) as

$$\mathcal{L} = \frac{1}{4\pi} K_{IJ} \epsilon^{\lambda\mu\nu} a_{I\lambda} \partial_\mu a_{J\nu} - \frac{e}{2\pi} \tau_I \epsilon^{\lambda\mu\nu} A_\lambda \partial_\mu a_{I\nu} \tag{42}$$

where a^1 and a^2 are internal gauge fields and A is external electro-magnetic field. $\tau_1 = \tau_2 = 1$. The charge carried by an anyon labeled by l can be calculated from

$$q_l = \tau^T K^{-1} l \tag{43}$$

in units of e^- and we can check explicitly that the e and m anyons both carry half charge with $\tau = (1, 1)$.

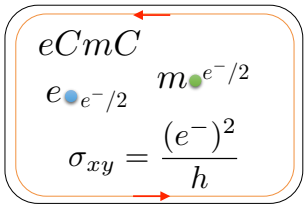

Figure 8: The $eCmC$ SF pattern: in 2D Z_2 topological state if both the e and m anyon carry half charge under charge conservation symmetry, the system has nonzero Hall conductance, hence explicitly breaks time reversal symmetry.

However, if in addition to charge conservation symmetry time reversal symmetry is also required, this SF pattern becomes anomalous. At first sight, it is not easy to see why this is the case, because the SF pattern seem to have no particular contradiction to time reversal symmetry. To see the anomaly, suppose that we can realize the theory described in Eq.42 in 2D with both charge conservation and time reversal symmetry. Imagine putting it on a disc with boundary, as shown in Fig.8. The Hall conductivity can be calculated from

$$\sigma_{xy} = \tau^T K^{-1} \tau \tag{44}$$

in units of $(e^-)^2/h$ and in this case $\sigma_{xy} = 1$. That is to say, there is a chiral edge mode going around the boundary, which explicitly violates time reversal symmetry. Therefore, we get a contradiction and the $eCmC$ SF pattern is not possible in 2D systems with time reversal symmetry. That is, with time reversal symmetry $eCmC$ is an anomalous SF pattern, even though it is consistent.

The $eCmC$ SF pattern provides an example where anomalies under time reversal symmetry can be detected by looking for chiral edge modes on the boundary. Anomalies with unitary symmetries, on the other hand, can only be revealed with more sophisticated methods. In the following sections, we are going to discuss various anomaly detection methods which allow us to see the anomaly in

1. $eCmT$ – Z_2 topological order with $U(1)$ spin conservation and time reversal symmetry (the two symmetries commute); e carries half spin, m carries integer spin; e is a time reversal singlet, m is a time reversal doublet.

2. Z_2 topological order with $Z_2 \times Z_2$ symmetry; e transforms as $i\sigma_z$, σ_x under the two Z_2's; m transforms as I, $i\sigma_y$ under the two Z_2's. (σ_x, σ_y, σ_z are Pauli matrices.)

3. Projective semion – chiral semion topological order with $Z_2 \times Z_2$ symmetry; the semion transforms as σ_x, σ_z under the two Z_2's.

6.2 Gauging and anomaly detection

The gauging procedure we discussed above plays an important role in detecting anomalies with unitary symmetries. If we have an SF pattern with the anyons transforming in a potentially fractional way under global symmetry, we can try to gauge the unitary part of the symmetry and obtain a new topological state.

How is this related to anomaly detection of SF patterns? If we know that certain SF pattern can be realized by a 2D lattice model, we can apply this procedure and find the expanded topological order starting from the original SF pattern. But of course in many case, we do not know if the assumption is true. In fact, this is exactly what we are trying to determine. What can help us, is a close connection between the original SF pattern and the expanded topological order if the gauging process can be carried through. Partial information about the expanded topological order, including its anyon types, part of their fusion rules and braiding statistics, can be determined from the SF pattern alone, without specific knowledge about its lattice realization. From this information one can determine if the gauging process can be carried through, resulting in a consistent expanded topological order. In some cases, however, we can see that there are inconsistencies in the gauging process, preventing the gauging process from completing. Such an obstruction to gauging indicates the existence of anomaly in the original SF pattern. This is the underlying logic behind the methods we describe in the following sections, where different methods provide different ways to reveal inconsistencies in the gauging process.

One important piece of information about the expanded topological order that can be extracted from the SF pattern is the fusion rules of gauge fluxes. Gauge fluxes are excitations in the gauged theory that violate the B_p term (the zero flux rule), but to determine their fusion rules it suffices to think in terms of the ungauged Hamiltonian H[2, 53].

To understand this relation, we can go back to the Ising paramagnet model on a square lattice. Suppose that we have both the Ising coupling term $\sigma_i^z\sigma_j^z$ and the transverse field term σ_i^x in the Hamiltonian. In the gauged Hamiltonian, these two terms become $\sigma_i^z\tau_{ij}^z\sigma_j^z$ and σ_i^x respectively. Now we do a 'gauge fixing' procedure in the ground state to remove the dynamics of the gauge field and retain only one particular configuration satisfying the no flux constraint B_p term. One simple choice is such that the gauge field is in the $\sigma^z = 1$ state (labelled by 0) on all links. The B_p terms are satisfied on all plaquettes. The A_v terms, which generate the dynamics of the gauge field, are violated as a result of gauge fixing. With this configuration of gauge field, the gauged Hamiltonian reduces back to the original Ising Hamiltonian with $\sigma_i^z\sigma_j^z$ and σ_i^x terms.

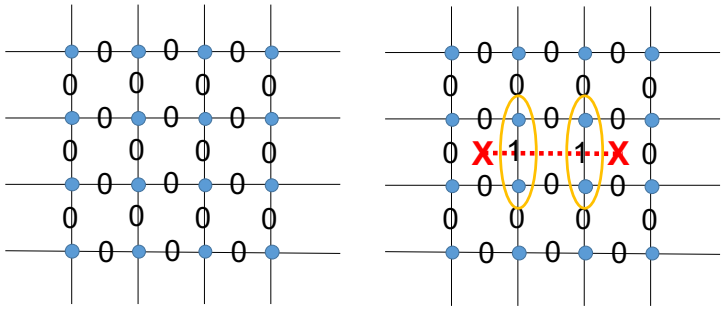

Figure 9: (left) Gauge fixing of zero flux configuration (right) Gauge fixing with a pair of fluxes (red crosses). Hamiltonian terms across the symmetry defect line (red dotted line) are conjugated by symmetry action on one side of the defect line.

Now suppose we create two gauge fluxes as shown in Fig.9. This can be achieved by flipping the gauge field to the $\sigma^z = -1$ state (labelled by 1) along the symmetry defect line (red dotted line). The B_p terms are satisfied everywhere except for the two end points of the symmetry defect line where the gauge fluxes reside (red crosses). With this configuration of gauge field, the $\sigma_i^z\tau_{ij}^z\sigma_j^z$ term becomes $-\sigma_i^z\sigma_j^z$ (orange circle) along the symmetry defect line and $\sigma_i^z\sigma_j^z$ everywhere else.

Such a change in the Hamiltonian ($\sigma_i^z\sigma_j^z$ to $-\sigma_i^z\sigma_j^z$ along the symmetry defect line) can be induced

by taking all Hamiltonian terms across the symmetry defect line and conjugating with symmetry action on one side of the symmetry defect line. The σ_i^x terms remain invariant and the $\sigma_i^z\sigma_j^z$ terms get a minus sign along the symmetry defect line. The ends of the symmetry defect line are then called the symmetry fluxes. Upon gauging, i.e. reintroducing dynamics of the gauge field, they become deconfined anyonic gauge flux excitations of H'.

For a general symmetry group G, by examining the symmetry fluxes Ω_g of H, we will show that they obey the 'projective' fusion rule

$$\Omega_{g_1} \times \Omega_{g_2} = a_{g_1,g_2}\Omega_{g_1 g_2} \tag{45}$$

which descends into the fusion rules of the gauge fluxes upon gauging. As we are going to see, this 'projective' fusion rule follows from the local projective symmetry action of a SF pattern given in Eq.11.

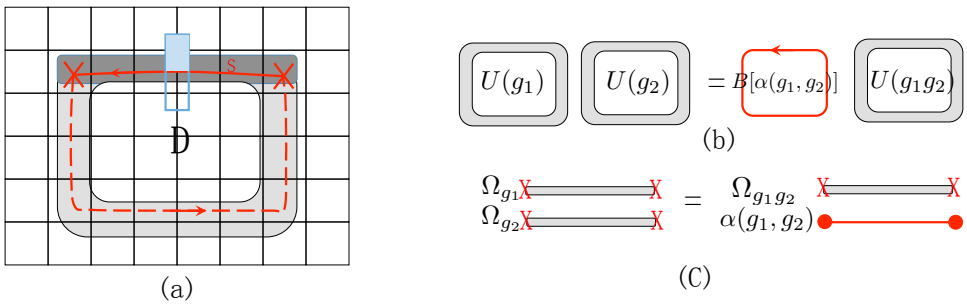

Figure 10: (a) A pair of symmetry fluxes (red crosses) can be created at the end of a symmetry defect line s (solid red line) by conjugating Hamiltonian terms across s (e.g. the one in the blue box) with symmetry on one side of s. A full braiding of the symmetry fluxes around region D is equivalent to applying symmetry locally to D and the change in the ground state can be induced by applying unitary $U(g)$ along the boundary of D (grey region). (b) $U(g)$ forms a projective representation of the symmetry. This is the same as Fig.5 (b) except that we have made it clear that $U(g)$ acts only along the boundary of D. (c) The symmetry fluxes hence satisfy a projective fusion rule as given in Eq.45.

Suppose that certain SF pattern can be realized in a lattice model as shown in Fig.10. We can insert a symmetry defect line s of $g \in G$ (solid red line in Fig.10) by taking the Hamiltonian terms which are bisected by this line (for example the term in the blue box) and conjugate them by symmetry operator on the lattice sites to one side of the line (the shaded blue region).

$$h_i \to \left(\prod_{k\in r.h.s.} M_k(g)\right) h_i \left(\prod_{k\in r.h.s.} M_k^{-1}(g)\right) \tag{46}$$

Here $r.h.s.$ stands for the right hand side of the defect line (or equivalently we can conjugate with $M_k(g^{-1})$ on the left hand side of the defect line). The terms which are not bisected by the defect line remain invariant. Near the end points – the symmetry fluxes marked by red crosses in Fig.10 – there may be terms that are only partially bisected by the defect line, so it is ambiguous how to change them. But this ambiguity is not a problem, because we are only interested in how things change along the middle part of the defect line. As the Hamiltonian is changed along s, the ground state is also changed, but only within a finite width along s (the dark grey region) due to the short range correlation in the state. Such a change in the ground state can be induced by applying a unitary operator $U^s(g)$ to the dark grey region along s and we can think of this $U^s(g)$ as the string

operator that creates a pair of symmetry fluxes and moves them around. An important difference between symmetry fluxes and anyons is that the symmetry fluxes are confined, i.e. the ground state changes along the full length of s and costs an amount of energy (in terms of the original H) that is proportional to the length of s.

Now imagine creating a pair of symmetry fluxes, braiding them around region D while changing the Hamiltonian along the way, and finally annihilating them (complete the circle along the dashed red line). After this full braiding process, all the Hamiltonian terms across the boundary of D get conjugated by symmetry on one side while the terms inside and outside of D remain invariant. The same change in Hamiltonian can be induced by applying symmetry locally to region D ($\prod_{k\in D} M_k(g)$): the terms inside D remain unchanged as they are invariant under global symmetry; the terms outside of D remain unchanged as they are not acted upon; the terms across the boundary of D get conjugated by symmetry on one side. Correspondingly, the change in the ground state can be induced by applying $\prod_{k\in D} M_k(g)$ to the region D. Therefore, braiding a pair of symmetry fluxes around a region corresponds to applying symmetry locally to that region.

On the other hand, the same change can be induced by applying a unitary string operator $U(g)$ along the boundary of D (the grey region in Fig.10). Note that $U(g)$ is very different from $\prod_{k\in D} M_k(g)$ as it has no action deep inside D, although applying them to the ground state induces the same change. In fact, this $U(g)$ is exactly the local symmetry action we discussed in section 4 which satisfies the projective composition rule as given in Eq.11, while the composition of $\prod_{k\in D} M_k(g)$ is not projective (because the composition of each $M_k(g)$ is not projective). Therefore, $U(g)$ carries the important information about the SF pattern while $\prod_{k\in D} M_k(g)$ does not. Eq.11 is saying that applying $U(g_1)$ and $U(g_2)$ is equivalent to applying $U(g_1g_2)$ up to the braiding of anyon $a(g_1, g_2)$ around the region D. This has to be the case because applying $U(g_1)U(g_2)U^{-1}(g_1g_2)$ to the Hamiltonian results in the same Hamiltonian, therefore the state can change at most by a phase factor. As $U(g_1)U(g_2)U^{-1}(g_1g_2)$ acts as a loop operator around region D, the phase factor can be induced by braiding an abelian anyon around D. On the other hand, from the fact that $U(g)$ implements the braiding of symmetry flux Ω_g around region D, we can further deduce that the fusion of Ω_{g_1} and Ω_{g_2} is equivalent to $\Omega(g_1g_2)$ up to $a(g_1, g_2)$, as shown in Eq. 45 and Fig.10 (c). Such a projective fusion rule among symmetry fluxes is the first step in several of the anomaly detection methods described below.

6.3 Flux Fusion

The flux fusion method discussed in [22] can be used to detect anomalies in for example the $eCmT$ SF pattern. The $eCmT$ SF pattern exists in systems with a Z_2 topological order with anyons $\mathbb{I}$, e, m and $f = e \times m$. Besides that, the system has charge conservation and time reversal symmetry $G = U(1) \times Z_2^T$. Note that here the charge conservation part is in direct product with the time reversal part, which means that the $U(1)$ charge gets reversed under time reversal. Therefore, it is better to think of the $U(1)$ part of the symmetry as spin conservation around the z axis, which reverses direction under time reversal.

The possibilities for symmetry fractionalization include fractional charges under $U(1)$ and Kramer doublet under time reversal ($\mathcal{T}^2 = -1$). In the $eCmT$ case we consider the situation where e carries half charge while m carries integer charge, e is a time reversal singlet while m transforms as a Kramer doublet. The consistency condition of the SF pattern is satisfied implicitly with f carrying half charge and transforming as a Kramer doublet.

In the first step of the anomaly test, we introduce symmetry flux of the $U(1)$ part of the symmetry and study its projective fusion rule (hence the name flux fusion). As e has half charge while m has integer charge, we can conclude that

$$\Omega_\pi \times \Omega_\pi = m \quad \text{or} \quad a(\pi, \pi) = m \tag{47}$$

In the second step, we ask the question: how does Ω_π transform under time reversal symmetry? First of all, we observe that time reversal does not change the amount of flux, because time reversal commutes with $U(1)$ rotations. Therefore, Ω_π transforms either as a time reversal singlet or a Kramers doublet. But this is in contradiction to m being a Kramers doublet because whether Ω_π is a time reversal singlet or doublet, the composite $\Omega_\pi \times \Omega_\pi = m$ must be a singlet. We have thus found that $eCmT$ is an anomalous fractionalization pattern.

The flux fusion method hence consists of 1. find the projective fusion rule of symmetry fluxes 2. examine whether symmetry fractionalization on the symmetry fluxes can be consistent with the fusion rule. It applies to a variety of situations including those with time reversal and spatial symmetries, but it is also restricted and does not apply when, for example, the symmetry flux type is changed under symmetry transformation.

In [36, 58, 57, 59], anomalies in SF patterns with $U(1)$ symmetry are detected using a 'monopole tunneling' method. Imagine tunneling a monopole through the 2D system and leaving behind a 2π flux. If the 2π flux carries projective symmetry number or statistics, then the quantum number of the monopole will change in a nontrivial way after tunneling, hence indicating anomaly. [36] first used this method to show the anomaly of the $eCmC$ state where the 2π flux is a fermion (unless there is an odd Hall conductance). In [58], it was shown that for $eCmT$ the 2π flux is a Kramer doublet and hence nontrivial. The flux fusion method is equivalent to this method when the symmetry flux inserted is a $U(1)$ flux.

6.4 Conflicting Symmetries

In [11] and [27], it was proposed that anomalies in SF patterns with $G_1 \times G_2$ type of symmetry may be detected through the 'conflict' between G_1 and G_2 which is revealed through the breaking of G_2 by gauging G_1. One example discussed in [11, 3] has Z_2 topological order and $Z_2^A \times Z_2^B$ unitary symmetry with group elements $\{I, g_A, g_B, g_A g_B\}$. The anyons transform as

$$e : U_e(g_A) = i\sigma_z, U_e(g_B) = \sigma_x; \quad m : U_m(g_A) = I, U_m(g_B) = i\sigma_y \tag{48}$$

The f anyon transforms as e and m combined, so the SF pattern is consistent. The fact that both e and m transform nontrivially under the symmetry lead to potential anomaly[26].

If we look at the two Z_2 symmetry subgroups individually, their actions are simple and not anomalous. For example, under the Z_2^A subgroup (generated by g_A), m transforms trivially while e carries half charge ($(U_e(g_A))^2 = -I$). Such a symmetry action can be realized in a strictly 2D system. Correspondingly we can fully gauge the Z_2^A subgroup and obtain a larger topological order. After gauging, the Z_2^B part remains a global symmetry of the system and acts on the anyons in the larger topological order. The 'conflict' between Z_2^A and Z_2^B, and hence the anomaly of the SF pattern, is detected through the observation that Z_2^B does not act on the larger topological order in a consistent way.

In particular, gauging Z_2^A results in a Z_4 topological order with elementary gauge charge e_4 ($e_4^4 = \mathbb{I}$) and elementary gauge flux m_4 ($m_4^4 = \mathbb{I}$). e_4 and m_4 has a mutual statistics of i. e_4 comes from the e anyon of the original Z_2 topological order; $e_4^2 = c$ is the symmetry charge of the Z_2^A symmetry; m_4 comes from the symmetry flux Ω_A of Z_2^A; $m_4^2 = m$ is the m anyons of the original Z_2 topological order.

In the next step, one can ask how the Z_2^B symmetry acts on the Z_4 topological order. Because in the original SF pattern, $U_e(g_B) = \sigma_x$ flips between the two components of e which differ by a -1 under the action of $U_e(g_A)$ (one with eigenvalue i and one with $-i$), in the gauged theory g_B exchanges e_4 and $e_4 c = e_4^3$. In order to keep the statistics of the Z_4 topological order invariant, g_B has to exchange m_4 and m_4^3. However, this is not consistent with the fact that $m = m_4^2$ carries half charge under g_B. In order to see this, we need the consistency condition of SF patterns when anyon types are changed under the symmetry. We did not discuss this in this review, although the result in section4 can be generalized directly as shown in [2, 53]. In [11], the SF pattern and the gauging procedure was discussed using the Chern-Simons formalism and it was explicitly shown that the Z_2^B symmetry action is not consistent with the Z_4 topological order obtained after gauging Z_2^A.

6.5 Gauging Obstruction

A powerful mathematical method exists to detect anomalies with unitary on-site symmetries. This is discussed in [40] as the 'obstruction to the extension of a braided fusion category by a finite group'. In [7], the projective semion example was used to illustrate this method.

The projective semion example has the topological order of a chiral semion theory, whose only nontrivial anyon s has topological spin i. The system also has unitary $Z_2 \times Z_2$ symmetry with group elements $\{I, g_x, g_y, g_z\}$. Four possible SF patterns on the semion are:

$$\begin{array}{lll} PS_0: & U_s(g_x) = i\sigma_x, & U_s(g_y) = i\sigma_y, \quad U_s(g_z) = i\sigma_z \\ PS_X: & U_s(g_x) = i\sigma_x, & U_s(g_y) = \sigma_y, \quad U_s(g_z) = \sigma_z \\ PS_Y: & U_s(g_x) = \sigma_x, & U_s(g_y) = i\sigma_y, \quad U_s(g_z) = \sigma_z \\ PS_Z: & U_s(g_x) = \sigma_x, & U_s(g_y) = \sigma_y, \quad U_s(g_z) = i\sigma_z \end{array} \tag{49}$$

Correspondingly, the symmetry fluxes fuse projectively as

$$\begin{array}{ll} PS_0: & a(X,X) = s, a(Y,Y) = s, a(Z,Z) = s \\ & a(X,Y) = a(Y,Z) = a(Z,X) = s, a(Y,X) = a(Z,Y) = a(X,Z) = \mathbb{I} \\ PS_X: & a(X,X) = s, a(Y,Y) = \mathbb{I}, a(Z,Z) = \mathbb{I} \\ & a(X,Y) = a(Y,Z) = a(Z,X) = s, a(Y,X) = a(Z,Y) = a(X,Z) = \mathbb{I} \\ PS_Y: & a(X,X) = \mathbb{I}, a(Y,Y) = s, a(Z,Z) = \mathbb{I} \\ & a(X,Y) = a(Y,Z) = a(Z,X) = s, a(Y,X) = a(Z,Y) = a(X,Z) = \mathbb{I} \\ PS_Z: & a(X,X) = \mathbb{I}, a(Y,Y) = \mathbb{I}, a(Z,Z) = s \\ & a(X,Y) = a(Y,Z) = a(Z,X) = s, a(Y,X) = a(Z,Y) = a(X,Z) = \mathbb{I} \end{array} \tag{50}$$

Now, if the symmetry in the projective semion theory can be consistently gauged, we should be able to define for the fluxes not only the projective fusion rules but also the braiding and fusion statistics involved with exchanging two fluxes or fusing three of them in different orders. These statistics cannot be chosen arbitrarily, but have to satisfy certain consistency conditions[2]. Failure to satisfy these consistency conditions reveals the anomaly in the SF pattern. We are not going

to explain the reasoning which led to the conclusion in [40] but only to quote that, to determine whether these consistency conditions can be satisfied, it suffices to calculate the following quantity

$$\begin{aligned}\nu(f,g,h,k) = \quad & R_{a(h,k),a(f,g)} F_{a(g,h),a(f,gh),a(fgh,k)} F^{-1}_{a(g,h),a(gh,k),a(f,ghk)} F_{a(f,g),a(h,k),a(fg,hk)} \\ & F^{-1}_{a(f,g),a(fg,h),a(fgh,k)} F_{a(h,k),a(g,hk),a(f,ghk)} F^{-1}_{a(h,k),a(f,g),a(fg,hk)}\end{aligned} \tag{51}$$

The F and R symbols depend on the anyon coefficient of the projective fusion rule of the symmetry fluxes and their value are determined from the semion topological order. $\nu(f,g,h,k)$ is a phase factor that depends on four group elements $f,g,h,k \in G$. However, in some cases it is possible that $\nu(f,g,h,k)$ can actually be generated from a phase factor μ which depends only on three group elements as

$$\nu(f,g,h,k) = \mu(g,h,k)\mu^{-1}(fg,h,k)\mu(f,gh,k)\mu^{-1}(f,g,hk)\mu(f,g,h) \tag{52}$$

The powerful conclusion of [40] is that: if this is the case, the SF pattern is not anomalous and the gauging process can go through. However, if this is not true, that is if $\nu(f,g,h,k)$ cannot be decomposed as in Eq.52, then the SF pattern is anomalous and there is obstruction to the gauging procedure. If we do this calculation for the projective semion SF pattern listed above, we can find that PS_0 is non-anomalous and PS_X, PS_Y, PS_Z are anomalous.

This 'Gauging Obstruction' method hence provides a generic tool for detecting anomalies in SF patterns with unitary symmetries. It is possible that this method can be generalized to anti-unitary symmetries[7], although the idea of 'gauging' applies most naturally to unitary symmetries.

7 Non-anomalous SF pattern as 2D spin liquid

Combining the consistency condition and the anomaly detection methods, we can now try to enumerate all SF patterns that can be realized in strictly 2D models with a given topological order and given global symmetry. In section 7.1, we review one such effort for Kagome lattice chiral spin liquid – a system with chiral semion topological order and symmetries common to a spin model on Kagome lattice (spin rotation, lattice symmetry, etc). Which one of these possible SF patterns is actually realized in the physically realistic models, like the nearest neighbor Heisenberg model? To answer this question, we need to be able to detect SF patterns through numerical or experimental probes. Some of the proposed probing methods are reviewed in section 7.2 and section 7.3 respectively.

7.1 Classification Example

[12] and [64] considered the classification of chiral spin liquid on the Kagome lattice. The chiral spin liquid contains one nontrivial anyon – the semion s, which can carry fractional representations of $SO(3)$ spin rotation, translation and plaquette centered inversion symmetry. While in a chiral spin liquid time reversal and reflection symmetries are individually broken, their combined action can still be preserved, under which the semion can transform projectively. It was found in [12] and [64] that in the physically interesting case of an odd number of spin 1/2s per unit cell, there is only one non-anomalous SF pattern for the chiral spin liquid.

First, it was proven that in a lattice with an odd number of spin 1/2s per unit cell, at least one anyon has to carry half integer spin[10]. In this case, it has to be the semion. Here we want to

comment that half integer spin is a nontrivial fractionalization pattern for the anyons even though the system is composed of half integer spins per lattice site. This is because, as long as the Hilbert space on each lattice site is not a direct sum of half integer and integer spins, global excitations (the difference between excited state and ground state) always carry integer spin. Only fractional excitations like the anyons can carry half integer spins.

In the next step, fractional quantum numbers are determined for the semion under translation symmetry T_x, T_y, inversion symmetry I_v and the combined action of reflection and time reversal R_x, R_y. It was found that the only non-anomalous possibility is that

$$U(I_v)^2 = s, U(T_x)U(T_y)U(T_x^{-1})U(T_y^{-1}) = s, U(R_x)^2 = s, U(R_y)^2 = s \tag{53}$$

which is saying that, for example, applying inversion (I_v) twice on the semion results in the phase factor of -1(the braiding statistics between two semions). Therefore, the SF pattern of the chiral spin liquid on Kagome lattice is completely fixed by the consistency condition and the anomaly free condition.

7.2 Numerical Probe

In other types of spin liquids (with different topological order or lattice symmetry), usually more than one SF pattern is potentially realizable[31, 30, 33, 65, 43, 4, 29, 42]. To determine which one is actually realized in a specific model, one can perform tests in numerical simulations, as discussed in [25, 12, 63, 60, 45, 64, 47].

A useful geometry for this purpose is the cylinder, as shown in Fig.11, with periodic boundary condition in the y direction and open boundary condition in the x direction. Consider the situation where the circumference along the y direction is finite while the length along the x direction is infinite. The 2D topological state with symmetry is then effectively reduced to a 1D gapped state with symmetry, with 1D symmetry protected topological order. This process is called 'dimensional reduction'.

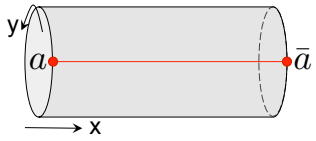

Figure 11: Putting the 2D system on a cylinder with finite circumference effectively reduces the system to 1D; creating a pair of anyons a and $\bar{a}$ at the two ends of the cylinder can change the symmetry protected topological order of the 1D state which can be measured to determine the SF pattern of a.

Now to detect symmetry fractionalization, one can create a pair of anyons a and $\bar{a}$ and bring them to the two ends of the cylinder. This process can change the symmetry protected topological order of the dimensional reduced system and the SF pattern of a is encoded in the change of the edge state of the 1D system. By measuring the symmetry protected topological order of the dimensional reduced system with, e.g., nonlocal order parameters[41, 18], one can determine the SF pattern of different anyons.

7.3 Experimental Probe

In fqH systems, the fractional charge carried by the anyons has been directly measured through shot-noise and local tunneling experiements[61, 13, 48, 32]. For spin liquids, candidate systems have been identified in organic Mott insulator κ-(BEDT-TTF)$_2$Cu$_2$(CN)$_3$[52] and herbertsmithite ZnCu$_3$(OH)$_6$Cl$_2$[20] etc. The nonexistence of magnetic order in these materials at very low temperature gives strong evidence that they are in a spin liquid state[19]. Can we obtain more direct evidence for the existence of a spin liquid by, for example, identifying the SF pattern? Several proposals have been made to address this issue.

[51] discussed different ways to detect spin charge separation in a spin liquid. In particular, in a superconductor – insulator – superconductor junction, if the insulator contains chargons – spinless charge e^- bosons, the ac Josephson current obtained by applying a dc voltage V across the junction will have an oscillating component at frequency $\omega = e^-V/\hbar$ in addition to the component at $\omega = 2e^-V/\hbar$. Similarly, the tunneling conductance into small superconducting islands across an insulating barrier behaves differently if the insulating barrier has spin-charge separation. With non-fractionalized insulating barrier, the tunneling conductance vary with the total charge on the island with a period of $2e^-$. If the the barrier contains chargons, the period becomes e^-.

More recently, [1] proposed that spin-charge separation can be directly measured by tunneling electrons into the spin liquid through suitably chosen boundary state. In particular, if chargons (spinons) are condensed at the boundary, electrons can leave their charge (spin) behind and enter the spin liquid as a fractional particle. This can be detected through the oscillation of the local density of states of the tunneling electron with the applied voltage, which results from the coherent propagation of fractional particles across the spin liquid.

On the other hand, [15] discussed experimental signature of crystal momentum fractionalization in Z_2 spin liquid. For example, translation in the x and y direction can anti-commute on a spinon

$$U_e(T_x)U_e(T_y)U_e(T_x^{-1})U_e(T_y^{-1}) = -1 \tag{54}$$

That is, bringing the spinon around a plaquette in the square lattice results in a phase factor of -1. If this is the case, then [15] showed that the density of states of the two-spinon continuum in the spectrum has an enhanced periodicity. In particular, for any two spinon state $|a\rangle$, applying translation on only one of the spinon generates three other different states $U_{e_1}(T_x)|a\rangle$, $U_{e_1}(T_y)|a\rangle$, $U_{e_1}(T_x)U_{e_1}(T_y)|a\rangle$ with different lattice momentum but the same energy. Therefore, the density of states repeats itself four times in the Brillouin zone, which can be detected through neutron scattering experiments.

8 Anomalous SF pattern on surface of 3D systems

When the SF patterns are anomalous, they cannot be realized in strictly 2D systems. However, they are not completely impossible either. It was realized that they can be found on the surface of a 3D system and their anomaly is a reflection of the nontrivial order inside the 3D bulk, as shown in Fig.12. This connection was first pointed out in [54] and many examples have been worked out demonstrating this kind of bulk-boundary correspondence. We review several interesting cases in this section, with anomalous SF pattern on the surface and symmetry protected topological order in the bulk.

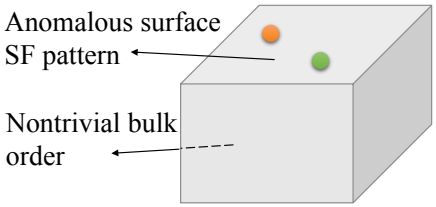

Figure 12: Anomalous SF patterns can be realized on the surface of a 3D system and their anomaly is a reflection of the nontrivial order in the 3D bulk.

8.1 Bosonic Topological Insulator

First, it was realized[54, 58] that the $eCmC$ SF pattern with time reversal discussed in section 6.1 can be realized on the surface of a 3D bosonic topological insulator. Being on the surface of a 3D system, it avoids the contradiction discussed in section 6.1 where the nonzero Hall conductance on the edge explicitly breaks time reversal. This is due to a simple, yet powerful, geometric observation that the 2D boundary of a 3D bulk does not have a boundary of its own. Therefore, we will not be able to observe the nonzero Hall conductance and there is no contradiction to the system being time reversal invariant. On the other hand, its existence as the 2D surface indicates special order in the 3D bulk, even though the anyons only live on the surface and cannot tunnel into the bulk. In particular it was shown[36] that the monopole in the 3D bulk is a fermion – the 'statistical Witten effect', indicating that the bulk state cannot be smoothly connected to a product state without breaking charge conservation and time reversal symmetry. The bulk state is the so-called 'Bosonic topological insulator' , following the terminology of fermionic topological insulators[17, 38, 46].

8.2 Bosonic $Z_2 \times Z_2$ symmetry protected topological phases

The projective semion SF patterns discussed in section 6.5 are realized on the surface of 3D bosonic symmetry protected topological phases with $Z_2 \times Z_2$ symmetry. It was shown in [7] that the PS_X, PS_Y and PS_Z SF patterns are realized on the surface of three different nontrivial phases. A strong indication of the relation between the surface anomaly and the bulk symmetry protected topological order is that they are both characterized by $\nu(f, g, h, k)$ (Eq.51), the fourth cocycle of the group. This kind of bulk-boundary correspondence is expected to apply for all unitary groups[55]. Moreover, one of the 3D bosonic symmetry protected topological phases with time reversal symmetry seems to fit into this scheme as well whose surface can have Z_2 topological order with both e and m transforming under time reversal as a Kramer doublet[6]. If we use Eq.51 to compute $\nu(f, g, h, k)$, we would obtain the nontrivial cocycle related to the bulk order.

8.3 Fermionic Topological Insulator

It is of great interest to investigate what kind of SF pattern can exist on the surface of 3D fermionic topological insulator, whose bulk state has been realized experimentally[23, 24, 9]. [5, 56, 8, 37] addressed this question and found the following two answers: the T-Pfaffian state and the Pfaffian-anti-semion state. Table 13 summarizes the anyon content and the SF pattern of the two states.

The two states share the following common properties: 1. as surface states, they have both time

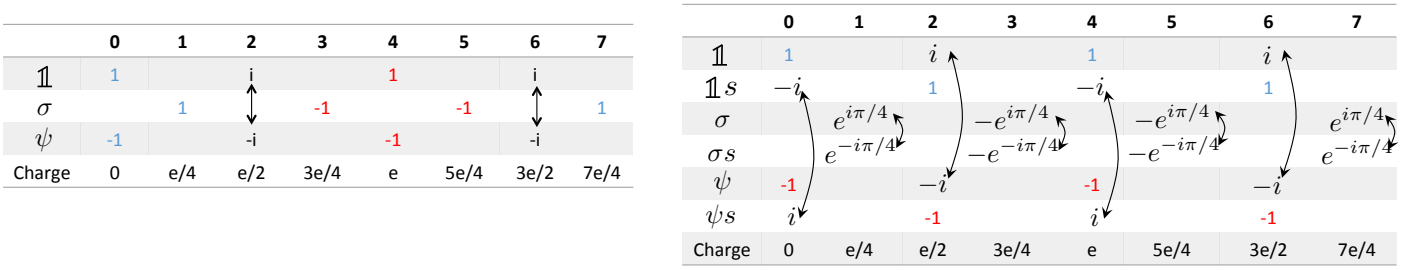

(a) T-Pfaffian

(b) Pfaffian anti-semion

Figure 13: The SF pattern on the surface of a 3D fermionic topological insulator. (a) the T-Pfaffian topological order is composed of an Ising sector ($\mathbb{I}$, σ, ψ) and a $U(1)_8$ sector ($0 \sim 7$) (b) the Pfaffian anti-semion topological order is composed of an Ising sector, an anti-semion sector (s) and a $U(1)_8$ sector. Entries in the table are topological spins of the anyon. Anyon pairs connected with an arrow are time reversal partners. Blue entries are for time reversal singlets while red entries are for time reversal doublets. The charge carried by the anyons are given in the last row of the tables.

reversal and charge conservation symmetry; 2. if realized in 2D with charge conservation symmetry, the system would have Hall conductance $\sigma_{xy} = \frac{(e^-)^2}{2h}$ and hence break time reversal symmetry; 3. if superconductivity is induced in the states, the π flux would host a Majorana zero mode. All these ensures that they are consistent with the bulk order. Although it suffices to have non-interacting electrons to realize the bulk state, to induce topological order and symmetry fractionalization on the surface, strong interaction is necessary. Exactly what kind of interaction is needed is still under investigation. By considering possible surface SF patterns, a complete classification of interacting topological insulators has been obtained[57]. Therefore, the study of SF pattern on the surface provides a useful strongly interacting perspective of symmetry protected topological phases. More discussions of these surface states can be found in [34, 50, 39]

8.4 Fermionic Topological Superconductor

[16, 35, 34, 62] studied the SF pattern possible on the surface of fermionic topological superconductors and the findings are listed in table 1. An interesting observation obtained from this analysis is that, when $\nu = 16$ (i.e. 16 copies of the elementary topological superconductor), the SF pattern becomes non-anomalous, implying that the $\nu = 16$ topological superconductor can be smoothly connected to a trivial s-wave superconductor. Such a connection is of course only possible with strong interaction, as in the non-interacting classification each integer ν corresponds to a different topological superconductor[49, 28]. A similar conclusion is reached for topological crystalline insulators where the $\nu = 8$ state is found to be trivial through the study of surface SF pattern[44].

References

[1] M. Barkeshli, E. Berg, and S. Kivelson. Coherent transmutation of electrons into fractionalized anyons. *Science*, 346(6210):722–725, 2014.

[2] M. Barkeshli, P. Bonderson, M. Cheng, and Z. Wang. Symmetry, defects, and gauging of topological phases. *ArXiv e-prints 1410.4540*, Oct. 2014.

TSc	Anyon content	Fusion rule	Topo spin	$\mathcal{T}$action	$\mathcal{T}^2$action
$\nu = 1(\text{mod } 2)$	$\mathbb{I}, S, Sf, f$	$S \times S = \mathbb{I} + S + Sf$	$\theta_S = i$	$S \leftrightarrow Sf$	
$\nu = \pm 2$	$\{\mathbb{I}, s\}\{\mathbb{I}, f\}$	$s \times s = \mathbb{I}$	$\theta_s = i$	$s \leftrightarrow sf$	$\mathcal{T}^2 = \pm i$ on s
$\nu = 4$	$\{\mathbb{I}, s_1\}\{\mathbb{I}, s_2\}\{\mathbb{I}, f\}$	$s_i \times s_i = \mathbb{I}, i = 1, 2$	$\theta_{s_{1,2}} = i$	$s_{1,2} \leftrightarrow s_{1,2}f$	$\mathcal{T}^2 = \pm i$ on $s_1,\ s_2$
$\nu = 8$	$\{\mathbb{I}, F_1, F_2, F_3\}\{\mathbb{I}, f\}$	$F_i \times F_i = \mathbb{I}, F_1 \times F_2 = F_3$	$\theta_{F_i} = -1$	$F_i \leftrightarrow F_i$	$\mathcal{T}^2 = 1$ on F_i

(55)

Table 1: The SF pattern on the surface of 3D fermionic topological superconductors. f is the Bogoliubov quasi-particle of the superconductor. $\mathcal{T}$ stands for time reversal.

[3] Z. Bi, A. Rasmussen, K. Slagle, and C. Xu. Classification and description of bosonic symmetry protected topological phases with semiclassical nonlinear sigma models. *Phys. Rev. B*, 91:134404, Apr 2015.

[4] S. Bieri, C. Lhuillier, and L. Messio. Projective symmetry group classification of chiral spin liquids. *Phys. Rev. B*, 93:094437, Mar 2016.

[5] P. Bonderson, C. Nayak, and X.-L. Qi. A time-reversal invariant topological phase at the surface of a 3d topological insulator. *Journal of Statistical Mechanics: Theory and Experiment*, 2013(09):P09016, 2013.

[6] F. J. Burnell, X. Chen, L. Fidkowski, and A. Vishwanath. Exactly soluble model of a three-dimensional symmetry-protected topological phase of bosons with surface topological order. *Phys. Rev. B*, 90:245122, Dec 2014.

[7] X. Chen, F. J. Burnell, A. Vishwanath, and L. Fidkowski. Anomalous symmetry fractionalization and surface topological order. *ArXiv e-prints 1403.6491*, Mar. 2014.

[8] X. Chen, L. Fidkowski, and A. Vishwanath. Symmetry enforced non-abelian topological order at the surface of a topological insulator. *Phys. Rev. B*, 89:165132, Apr 2014.

[9] Y. L. Chen, J. G. Analytis, J.-H. Chu, Z. K. Liu, S.-K. Mo, X. L. Qi, H. J. Zhang, D. H. Lu, X. Dai, Z. Fang, S. C. Zhang, I. R. Fisher, Z. Hussain, and Z.-X. Shen. Experimental realization of a three-dimensional topological insulator, bi2te3. *Science*, 325(5937):178–181, 2009.

[10] M. Cheng, M. Zaletel, M. Barkeshli, A. Vishwanath, and P. Bonderson. Translational symmetry and microscopic constraints on symmetry-enriched topological phases: a view from the surface. *ArXiv e-prints 1511.02263*, Nov. 2015.

[11] G. Y. Cho, J. C. Y. Teo, and S. Ryu. Conflicting symmetries in topologically ordered surface states of three-dimensional bosonic symmetry protected topological phases. *Phys. Rev. B*, 89:235103, Jun 2014.

[12] L. Cincio and Y. Qi. Classification and detection of symmetry fractionalization in chiral spin liquids. *ArXiv e-prints 1511.02226*, Nov. 2015.

[13] R. de Picciotto, M. Reznikov, M. Heiblum, V. Umansky, G. Bunin, and D. Mahalu. Direct observation of a fractional charge. *Nature*, 389(6647):162–164, 09 1997.

[14] A. M. Essin and M. Hermele. Classifying fractionalization: Symmetry classification of gapped F_2 spin liquids in two dimensions. *Phys. Rev. B*, 87:104406, Mar 2013.

[15] A. M. Essin and M. Hermele. Spectroscopic signatures of crystal momentum fractionalization. *Phys. Rev. B*, 90:121102, Sep 2014.

[16] L. Fidkowski, X. Chen, and A. Vishwanath. Non-abelian topological order on the surface of a 3d topological superconductor from an exactly solved model. *Phys. Rev. X*, 3:041016, Nov 2013.

[17] L. Fu, C. L. Kane, and E. J. Mele. Topological insulators in three dimensions. *Phys. Rev. Lett.*, 98(10):106803–, Mar. 2007.

[18] J. Haegeman, D. Pérez-García, Davidia, I. Cirac, and N. Schuch. Order parameter for symmetry-protected phases in one dimension. *Phys. Rev. Lett.*, 109:050402, Jul 2012.

[19] M. B. Hastings. Lieb-schultz-mattis in higher dimensions. *Phys. Rev. B*, 69:014431–, 2004.

[20] J. S. Helton, K. Matan, M. P. Shores, E. A. Nytko, B. M. Bartlett, Y. Yoshida, Y. Takano, A. Suslov, Y. Qiu, J.-H. Chung, D. G. Nocera, and Y. S. Lee. Spin dynamics of the spin-1/2 kagome lattice antiferromagnet zncu$_3$(oh)$_6$cl$_2$. *Phys. Rev. Lett.*, 98(10):107204–, Mar. 2007.

[21] M. Hermele. String flux mechanism for fractionalization in topologically ordered phases. *Phys. Rev. B*, 90:184418, Nov 2014.

[22] M. Hermele and X. Chen. Bosonic topological crystalline insulators and anomalous symmetry fractionalization via the flux-fusion anomaly test. *to appear*, 2015.

[23] D. Hsieh, D. Qian, L. Wray, Y. Xia, Y. S. Hor, R. J. Cava, and M. Z. Hasan. A topological dirac insulator in a quantum spin hall phase. *Nature*, 452(7190):970–974, Apr. 2008.

[24] D. Hsieh, Y. Xia, D. Qian, L. Wray, J. H. Dil, F. Meier, J. Osterwalder, L. Patthey, J. G. Checkelsky, N. P. Ong, A. V. Fedorov, H. Lin, A. Bansil, D. Grauer, Y. S. Hor, R. J. Cava, and M. Z. Hasan. A tunable topological insulator in the spin helical dirac transport regime. *Nature*, 460(7259):1101–1105, July 2009.

[25] C.-Y. Huang, X. Chen, and F. Pollmann. Detection of symmetry-enriched topological phases. *Phys. Rev. B*, 90:045142, Jul 2014.

[26] A. Kapustin and R. Thorngren. Anomalies of discrete symmetries in various dimensions and group cohomology. *ArXiv e-prints 1404.3230*, Apr. 2014.

[27] A. Kapustin and R. Thorngren. Anomalous discrete symmetries in three dimensions and group cohomology. *Phys. Rev. Lett.*, 112:231602, Jun 2014.

[28] A. Kitaev. Periodic table for topological insulators and superconductors. *AIP Conference Proceedings*, 1134(1):22–30, 2009.

[29] Y.-M. Lu. Symmetric Z_2 spin liquids and their neighboring phases on triangular lattice. *Phys. Rev. B*, 93:165113, Apr 2016.

[30] Y.-M. Lu and Y. Ran. z_2 spin liquid and chiral antiferromagnetic phase in the hubbard model on a honeycomb lattice. *Phys. Rev. B*, 84(2):024420–, July 2011.

[31] Y.-M. Lu, Y. Ran, and P. A. Lee. z_2 spin liquids in the s=1/2 heisenberg model on the kagome lattice: A projective symmetry-group study of schwinger fermion mean-field states. *Phys. Rev. B*, 83(22):224413–, June 2011.

[32] J. Martin, S. Ilani, B. Verdene, J. Smet, V. Umansky, D. Mahalu, D. Schuh, G. Abstreiter, and A. Yacoby. Localization of fractionally charged quasi-particles. *Science*, 305(5686):980–983, 2004.

[33] L. Messio, C. Lhuillier, and G. Misguich. Time reversal symmetry breaking chiral spin liquids: Projective symmetry group approach of bosonic mean-field theories. *Phys. Rev. B*, 87:125127, Mar 2013.

[34] M. A. Metlitski. S-duality of u(1) gauge theory with = on non-orientable manifolds: Applications to topological insulators and superconductors. *ArXiv e-prints 1510.05663*, Oct. 2015.

[35] M. A. Metlitski, L. Fidkowski, X. Chen, and A. Vishwanath. Interaction effects on 3d topological superconductors: surface topological order from vortex condensation, the 16 fold way and fermionic kramers doublets. *ArXiv e-prints 1406.3032*, June 2014.

[36] M. A. Metlitski, C. L. Kane, and M. P. A. Fisher. Bosonic topological insulator in three dimensions and the statistical witten effect. *arXiv:1302.6535*, 2013.

[37] M. A. Metlitski, C. L. Kane, and M. P. A. Fisher. Symmetry-respecting topologically ordered surface phase of three-dimensional electron topological insulators. *Phys. Rev. B*, 92:125111, Sep 2015.

[38] J. E. Moore and L. Balents. Topological invariants of time-reversal-invariant band structures. *Phys. Rev. B*, 75(12):121306–, Mar. 2007.

[39] D. F. Mross, A. Essin, and J. Alicea. Composite dirac liquids: Parent states for symmetric surface topological order. *Phys. Rev. X*, 5:011011, Feb 2015.

[40] D. N. Pavel Etingof and V. Ostrik. Fusion categories and homotopy theory. *QUANTUM TOPOLOGY*, 1(3):209–273, 2010.

[41] F. Pollmann and A. M. Turner. Detection of symmetry-protected topological phases in one dimension. *Phys. Rev. B*, 86:125441, Sep 2012.

[42] Y. Qi and M. Cheng. Classification of symmetry fractionalization in gapped 2 spin liquids classification of symmetry fractionalization in gapped 2 spin liquids. *ArXiv e-prints 1606.04544*, June 2016.

[43] Y. Qi, M. Cheng, and C. Fang. Symmetry fractionalization of visons in z_2 spin liquids. *ArXiv e-prints 1509.02927*, Sept. 2015.

[44] Y. Qi and L. Fu. Anomalous crystal symmetry fractionalization on the surface of topological crystalline insulators. *Phys. Rev. Lett.*, 115:236801, Dec 2015.

[45] Y. Qi and L. Fu. Detecting crystal symmetry fractionalization from the ground state: Application to F_2 spin liquids on the kagome lattice. *Phys. Rev. B*, 91:100401, Mar 2015.

[46] R. Roy. Topological phases and the quantum spin hall effect in three dimensions. *Phys. Rev. B*, 79(19):195322–, May 2009.

[47] I. P. M. S. N. Saadatmand. Symmetry fractionalization in the topological phase of the spin-1/2 j1-j2 triangular heisenberg model. *ArXiv e-prints 1606.00334*, June 2016.

[48] L. Saminadayar, D. C. Glattli, Y. Jin, and B. Etienne. Observation of the $e/3$ fractionally charged laughlin quasiparticle. *Phys. Rev. Lett.*, 79:2526–2529, Sep 1997.

[49] A. P. Schnyder, S. Ryu, A. Furusaki, and A. W. W. Ludwig. Classification of topological insulators and superconductors in three spatial dimensions. *Phys. Rev. B*, 78(19):195125–, Nov. 2008.

[50] N. Seiberg. Gapped boundary phases of topological insulators via weak coupling gapped boundary phases of topological insulators via weak coupling. *ArXiv e-prints 1602.04251*, Feb. 2016.

[51] T. Senthil and M. P. A. Fisher. Detecting fractions of electrons in the high-T_c cuprates. *Phys. Rev. B*, 64:214511, Nov 2001.

[52] Y. Shimizu, K. Miyagawa, K. Kanoda, M. Maesato, and G. Saito. Spin liquid state in an organic mott insulator with a triangular lattice. *Phys. Rev. Lett.*, 91(10):107001–, Sept. 2003.

[53] N. Tarantino, N. Lindner, and L. Fidkowski. Symmetry fractionalization and twist defects. *ArXiv e-prints 1506.06754*, June 2015.

[54] A. Vishwanath and T. Senthil. Physics of three-dimensional bosonic topological insulators: Surface-deconfined criticality and quantized magnetoelectric effect. *Phys. Rev. X*, 3:011016, Feb 2013.

[55] C. Wang, C.-H. Lin, and M. Levin. Bulk-boundary correspondence for three-dimensional symmetry-protected topological phases. *Phys. Rev. X*, 6:021015, May 2016.

[56] C. Wang, A. C. Potter, and T. Senthil. Gapped symmetry preserving surface state for the electron topological insulator. *Phys. Rev. B*, 88:115137, Sep 2013.

[57] C. Wang, A. C. Potter, and T. Senthil. Classification of interacting electronic topological insulators in three dimensions. *Science*, 343(6171):629–631, 2014.

[58] C. Wang and T. Senthil. Boson topological insulators: A window into highly entangled quantum phases. *arXiv:1302.6234*, 2013.

[59] C. Wang and T. Senthil. Time-reversal symmetric $u(1)$ quantum spin liquids. *Phys. Rev. X*, 6:011034, Mar 2016.

[60] L. Wang, A. Essin, M. Hermele, and O. Motrunich. Numerical detection of symmetry-enriched topological phases with space-group symmetry. *Phys. Rev. B*, 91:121103, Mar 2015.

[61] X. G. Wen. Chiral luttinger liquid and the edge excitations in the fractional quantum hall states. *Phys. Rev. B*, 41(18):12838–, June 1990.

[62] E. Witten. The "parity" anomaly on an unorientable manifold. *ArXiv e-prints 1605.02391*, May 2016.

[63] M. Zaletel, Y.-M. Lu, and A. Vishwanath. Measuring space-group symmetry fractionalization in z_2 spin liquids. *ArXiv e-prints 1501.01395*, Jan. 2015.

[64] M. P. Zaletel, Z. Zhu, Y.-M. Lu, A. Vishwanath, and S. R. White. Space group symmetry fractionalization in a chiral kagome heisenberg antiferromagnet. *Phys. Rev. Lett.*, 116:197203, May 2016.

[65] W. Zheng, J.-W. Mei, and Y. Qi. Classification and monte carlo study of symmetric z_2 spin liquids on the triangular lattice. *ArXiv e-prints 1505.05351*, May 2015.